PAIN® xxx (2013) xxx–xxx

PAIN®

www.elsevier.com/locate/pain

Reliable EEG responses to the selective activation of C-fibre afferents using a temperature-controlled infrared laser stimulator in conjunction with an adaptive staircase algorithm

Aleksandar Jankovski [a,b], Léon Plaghki [a], André Mouraux [a,*]

[a] Institute of Neuroscience (IONS), Université catholique de Louvain, Belgium
[b] Department of Neurosurgery, CHU Mont-Godinne, Université catholique de Louvain, Belgium

Sponsorships or competing interests that may be relevant to content are disclosed at the end of this article.

ARTICLE INFO

Article history:
Received 10 September 2012
Received in revised form 12 April 2013
Accepted 16 April 2013
Available online xxxx

Keywords:
Aδ-fibres
C-fibres
Laser-evoked potentials
Nociception
Pain
Reaction times
Staircase algorithm

ABSTRACT

Brain responses to the activation of C-fibres are obtained only if the co-activation of Aδ-fibres is avoided. Methods to activate C-fibres selectively have been proposed, but are unreliable or difficult to implement. Here, we propose an approach combining a new laser stimulator to generate constant-temperature heat pulses with an adaptive paradigm to maintain stimulus temperature above the threshold of C-fibres but below that of Aδ-fibres, and examine whether this approach can be used to record reliable C-fibre laser-evoked brain potentials. Brief CO_2 laser stimuli were delivered to the hand and foot dorsum of 10 healthy subjects. The stimuli were generated using a closed-loop control of laser power by an online monitoring of target skin temperature. The adaptive algorithm, using reaction times to distinguish between late detections indicating selective activation of unmyelinated C-fibres and early detections indicating co-activation of myelinated Aδ-fibres, allowed increasing the likelihood of selectively activating C-fibres. Reliable individual-level electroencephalogram (EEG) responses were identified, both in the time domain (hand: N2: 704 ± 179 ms, P2: 984 ± 149 ms; foot: N2: 1314 ± 171 ms, P2: 1716 ± 171 ms) and the time-frequency (TF) domain. Using a control dataset in which no stimuli were delivered, a Receiver Operating Characteristics analysis showed that the magnitude of the phase-locked EEG response corresponding to the N2-P2, objectively quantified in the TF domain, discriminated between absence vs presence of C-fibre responses with a high sensitivity (hand: 85%, foot: 80%) and specificity (hand: 90%, foot: 75%). This approach could thus be particularly useful for the diagnostic workup of small-fibre neuropathies and neuropathic pain.

1. Introduction

Provided that the peripheral conduction distance is sufficiently large, a brief and intense thermal stimulus applied onto the skin elicits sensations referred to as first and second pain [17]. This double sensation is related to the fact that the stimulus coactivates myelinated Aδ-fibre and unmyelinated C-fibre afferents [3], each having different conduction velocities [27,37]. Using such stimuli, laser-evoked brain potentials (LEPs) reveal components whose latencies (160 to 390 ms when stimulating the hand dorsum) are only compatible with the faster conduction velocity of Aδ-fibres [3].

However, several studies have shown that if C-fibres are activated in isolation, later LEP components are recorded at latencies compatible with C-fibre conduction velocities (750 to 1150 ms when stimulating the hand dorsum) [19,21,35]. Different approaches have been proposed to activate C-fibres selectively. Bromm et al. (1983) showed that prolonged pressure applied against a peripheral nerve can preferentially block the conduction of myelinated A-fibres [2]. Bragard et al. (1996) showed that thermal stimuli delivered using a very small surface area (eg, 0.15 mm^2) can increase the probability of selectively activating C-fibre afferents, which are thought to be more densely distributed in the epidermis than Aδ-fibre afferents [1,25]. Magerl et al. (1999) showed that low-intensity thermal stimuli can selectively activate C-fibre afferents having a lower thermal activation threshold than Aδ-fibre afferents [10,19]. Finally, Otsuru et al. (2009) [30] recently described a method relying on intraepidermal needle electrodes to selectively activate C-fibre free nerve endings using short trains of low-intensity pulses just above the detection threshold.

* Corresponding author. Address: Institute of Neuroscience (IONS), Université catholique de Louvain, 53, Avenue Mounier, B1200 Bruxelles, Belgium. Tel.: +32 2 764 9349; fax: +32 2 764 5360.
E-mail address: andre.mouraux@uclouvain.be (A. Mouraux).

0304-3959/$36.00
http://dx.doi.org/10.1016/j.pain.2013.04.032

Please cite this article in press as: Jankovski A et al. Reliable EEG responses to the selective activation of C-fibre afferents using a temperature-controlled infrared laser stimulator in conjunction with an adaptive staircase algorithm. PAIN® (2013), http://dx.doi.org/10.1016/j.pain.2013.04.032

Unfortunately, C-fibre event-related potentials obtained using these methods display a very small signal-to-noise ratio, and most importantly, these methods are technically challenging to implement, especially in a clinical setting. Hence, there is a general consensus that a simple and robust technique to activate C-fibre afferents selectively would constitute a highly needed clinical and research tool to assess C-fibre function in humans, for example, to characterise neuropathic pain or small-fibre neuropathies We examined whether reliable C-fibre LEPs could be recorded after stimulation of the hand and foot dorsum of healthy subjects using a CO_2 laser with closed-loop control of skin temperature [6]. The laser was used in conjunction with an adaptive paradigm relying on reaction times (RT) to identify responses related to the detection of Aδ- vs C-fibre input (ie, RTs with latencies compatible with the conduction velocity of myelinated Aδ- vs unmyelinated C-fibres). Thereby, target skin temperature was adjusted on a trial-by-trial basis, with the aim of increasing the likelihood of selectively activating C-fibres.

Furthermore, we hypothesised that the low signal-to-noise ratio of C-fibre LEPs could at least in part be due to an important amount of temporal jitter affecting the brain responses to C-fibre input, possibly due to the slow and variable conduction velocity of these afferents [4]. For this reason, we used a TF wavelet decomposition of single-trial EEG epochs to reveal activity that is induced by the stimulus, but not sufficiently stationary across trials to be revealed by conventional across-trial averaging in the time domain [18,21].

2. Methods

2.1. Participants

Ten healthy participants (3 women; 10 right-handed, aged 22 to 40 years) took part in the study. All participants were right handed. Before the experiment, they were familiarised with the sensory stimulus and RT task. Experimental procedures were approved by the Ethics Committee of the Université catholique de Louvain.

2.2. CO_2 laser stimulation of Aδ- and C-fibre nociceptors

Thermal stimuli were delivered to the left and right hand and foot dorsum, in separate blocks. The order of the blocks was randomised across participants. The stimuli consisted of 100-ms pulses of radiant heat, during which the temperature of the stimulated area was raised to a defined temperature (ranging between 32°C and 50°C) using a very steep 10-ms heating ramp and then maintained at that temperature for an additional 90 ms (Fig. 1). The stimuli were generated using a CO_2 laser stimulator with power that is regulated using a feedback control based on an online measurement of skin temperature at the site of stimulation (Laser Stimulation Device, SIFEC, Ferrière, Belgium) [6]. Conception of the laser was inspired by a similar feedback-controlled device developed by Meyer et al. (1976) [20]. Both devices are based on a closed-loop control of laser power by an online monitoring of skin temperature performed using a radiometer collinear with the laser beam. The present device allows production of temperature steps with rise rates greater than 350°C/s and pulse durations from 10 ms to 12 seconds. The heat source is a 25-W radiofrequency-excited CO_2 laser (Synrad 48-2; Synrad, Mukilteo, WA). Power control is achieved by pulse width modulation at 5-kHz clock frequency. The stimuli are delivered through a 10-m optical fibre. By vibrating this fibre at some distance from the source, a quasiuniform spatial distribution of radiative power within the stimulated area is obtained. At the end of the fibre, optics are used to collimate the beam. The optic used in the present study provided a 12-mm beam.

2.3. Adaptive stimulation algorithm to preferentially activate C-fibres

Because the thermal activation threshold of at least a fraction of C-fibre afferents (eg, C-warm receptors) is lower than that of Aδ-fibre afferents [3,6,24], it was expected that the skin temperature required to elicit Aδ-fibre responses would be higher than the skin temperature required to elicit C-fibre responses. Hence, we expected that selective activation of C-fibres could be achieved using intermediate target skin temperatures, exceeding the threshold of C-fibre afferents, but remaining below the thermal activation threshold of Aδ-fibres [6].

Participants were asked to respond as quickly as possible by pressing a button as soon as they perceived the stimulus. When stimulating the left hand, the left foot, and the right foot, the button was held in the right hand. When stimulating the right hand, the button was held in the left hand. RTs were measured relative to the onset of the thermal stimulus. Because the nerve conduction velocity of unmyelinated C-fibres is markedly lower than that of Aδ-fibres, these RTs were used to discriminate between responses triggered by Aδ- and C-fibre input. Taking into account peripheral conduction distance, a cut-off of 650 ms was used to discriminate between Aδ- and C-fibre responses when stimulating the hand dorsum [21], and a cut-off of 750 ms was used when stimulating the foot dorsum [23].

An adaptive stimulation paradigm was used to increase the likelihood of activating C-fibres in isolation, as follows (Fig. 1). The target temperature of the first stimulus was set to 41°C, ie, a skin temperature likely to be slightly above the thermal activation threshold of heat-sensitive C-fibre afferents, but below the thermal activation threshold of heat-sensitive Aδ-fibre afferents, previously estimated at 39.8°C ± 1.7°C and 46.9°C ± 1.7°C, respectively [6]. The temperature of each of the following test stimuli was determined by the participant's RT to the preceding stimulus. If the preceding stimulus was not detected, the temperature of the stimulus was increased by 1°C. If it was detected with an RT compatible with the conduction velocity of C-fibres (hand: RT $\geqslant$ 650 ms; foot: RT $\geqslant$ 750 ms), the stimulus was unchanged. If it was detected with an RT compatible with the conduction velocity of Aδ-fibres (hand: RT < 650 ms; foot: RT < 750 ms), the stimulus was decreased by 1°C. At each stimulated site, a total of 40 stimuli were delivered, with an interstimulus interval varying randomly (rectangular distribution) between 5 and 10 seconds.

2.4. EEG recording

The EEG was recorded using 64 Ag-AgCl electrodes placed on the scalp according to the international 10-10 system (Waveguard64 cap, Cephalon A/S, Nørresundby, Denmark). Scalp signals were recorded using an average reference. Impedance was kept below 10 kΩ. Ocular movements and eye blinks were recorded using 2 surface electrodes placed at the upper-left and lower-right sides of the right eye. The signals were amplified and digitized at a 1-kHz sampling rate [11].

2.5. Signal processing

All EEG signal processing steps were conducted using BV Analyzer 1.05 (Brain Products, Gilching, Germany), Letswave4 [22] and EEGLAB (http://sccn.ucsd.edu/eeglab). Continuous EEG signals were band-pass filtered (0.3 to 30 Hz) using a Butterworth zero-phase filter. Activities at higher frequencies (eg, gamma-band oscillations) were thus not explored in the present study. Continuous EEG signals were segmented into 3-second epochs ranging from −1 to +2 seconds relative to the onset of the stimulus (LEP dataset). After baseline correction (reference interval: −0.5 to 0 seconds), artifacts produced by eye blinks or eye movements were subtracted

Please cite this article in press as: Jankovski A et al. Reliable EEG responses to the selective activation of C-fibre afferents using a temperature-controlled infrared laser stimulator in conjunction with an adaptive staircase algorithm. PAIN® (2013), http://dx.doi.org/10.1016/j.pain.2013.04.032

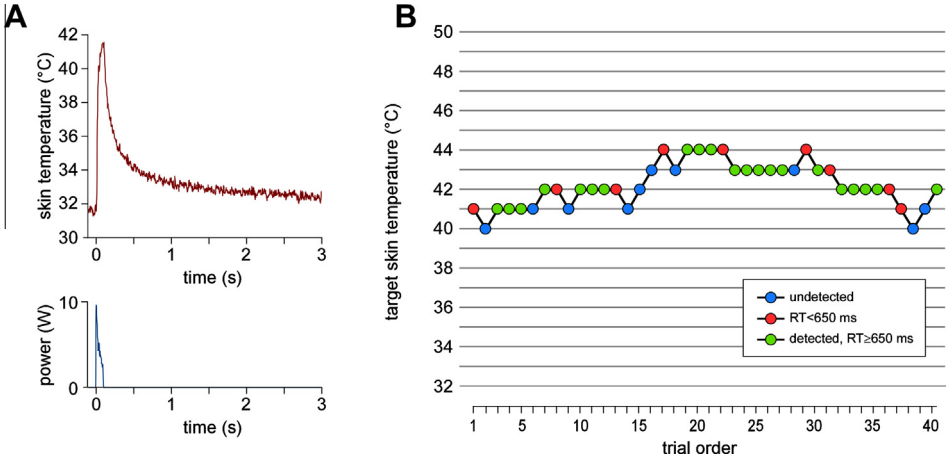

Fig. 1. (A) Constant-temperature heat pulse (heat ramp: 10 ms; total duration: 100 ms; target skin temperature: 42°C) generated by a CO_2 laser stimulator with a power output (blue curve) that is regulated continuously using a feedback loop based on an online measurement of target skin temperature (red curve). (B) In conjunction with a stimulation algorithm based on reaction time (RT), the stimulator was used to preferentially activate heat-sensitive C-fibre afferents. Blocks of 40 stimuli were delivered to each stimulation site. The figure represents the time course of a block applied onto the left hand in 1 representative subject. Within each block, the first stimulus was set to 41°C. If the preceding stimulus was not detected (blue), the target temperature of the following stimulus was increased by 1°C. If it was detected with an RT compatible with the conduction velocity of C-fibres (green), temperature was unchanged. If it was detected with an RT compatible with the conduction velocity of Aδ-fibres (red), temperature was decreased by 1°C.

using a validated method based on an Independent Component Analysis [13]. In addition, epochs with amplitude values exceeding ±100 μV (ie, epochs likely to be contaminated by an artifact) were rejected.

To evaluate the signal-to-noise ratio of the elicited EEG responses, an additional dataset was constructed by segmenting the EEG recordings from −4 to −1 seconds relative to the onset of the stimulus. This dataset, referred to as NOLEP, was expected to contain only background EEG activity, and was thus used to evaluate the ability to discriminate between presence vs. absence of C-fibre–related stimulus-evoked EEG responses.

2.6. Across-trial averaging in the time domain

For each dataset (LEP and NOLEP), separate average waveforms were computed for each subject and stimulation site (left hand, right hand, left foot, right foot). The obtained average waveforms are shown in Figs. 2 and 3.

2.6.1. Visual identification of C-fibre LEPs

For each stimulation site, 3 experienced observers were asked to identify the N2 and P2 components of C-fibre LEPs [26] within the LEP (Fig. 2) and NOLEP waveforms. The waveforms were presented in a blinded fashion. The N2 wave was defined as a negative peak maximal at the scalp vertex (electrode Cz), occurring between 500 and 1500 ms after stimulus onset. The P2 wave was defined as a positive peak also maximal at the scalp vertex, occurring between 500 and 2000 ms after stimulus onset [26]. The observers were asked (1) to determine whether or not the N2 and P2 waves were present, and if present, (2) to determine their latency and baseline-to-peak amplitude at electrode Cz.

Latencies and amplitudes of the N2 and P2 waves obtained after stimulation of the left and right hand and foot were compared using a 2-way repeated-measures ANOVA with side (left vs right) and extremity (hand vs foot) as experimental factors. Degrees of freedom were corrected using the Greenhouse-Geisser correction for violations of sphericity. When significant, post-hoc pairwise comparisons were performed using paired-sampled *t* tests. Significance level was set at $P < .05$.

2.6.2. Point-by-point statistical analysis of event-related potential (ERP) waveforms

To assess the group-level significance of the ERP waveforms obtained after stimulation of the hand and foot, a 1-sample *t* test against zero was performed, using each time point of the averaged waveforms recorded at each channel location. This yielded, for each stimulation site and each electrode location, the time intervals at which the ERP waveforms deviated significantly from baseline (Fig. 3).

2.6.3. Point-by-point statistical assessment of hemispheric lateralization

To assess the possible hemispheric lateralization of the ERP waveforms obtained after stimulation of the hand and foot [28], for each time point of the average waveforms, paired-sample *t* tests were performed using all pairs of scalp electrodes located left and right from the midline (eg, C1 vs C2, C3 vs C4) (Fig. 5). This yielded a time-varying scalp map of the regions displaying a significant hemispheric asymmetry.

2.7. Across-trial averaging in the TF domain

A TF representation based on the continuous Morlet wavelet transform of EEG epochs was used to characterize the amplitude of the recorded EEG signals as a function of time and frequency. Explored frequencies ranged from 1 to 31 Hz in steps of 0.3 Hz. The initial spread of the Morlet wavelet was set to $2.5/\pi\omega 0$ ($\omega 0$ being the central frequency of the wavelet) [21,22].

The TF transform was applied to each single EEG epoch. Single-trial matrices expressing signal amplitude as a function of time and frequency were then averaged across trials. This approach yielded TF maps of the average oscillation amplitude regardless of phase, and thus enhanced both phase-locked and non–phase-locked stimulus-induced changes in EEG oscillation amplitude (Fig. 6).

For each estimated frequency, single-subject TF maps were expressed relative to baseline (prestimulus interval ranging from −0.4 to −0.1 seconds relative to stimulus onset), as follows: $ER\%[t,-f] = (A[t,f] - R[f])/R[f]$, where A[t,f] corresponded to the estimated signal amplitude at latency t and frequency f; and R[f] corresponded the signal amplitude at frequency f, averaged within the prestimulus reference interval.

Please cite this article in press as: Jankovski A et al. Reliable EEG responses to the selective activation of C-fibre afferents using a temperature-controlled infrared laser stimulator in conjunction with an adaptive staircase algorithm. PAIN® (2013), http://dx.doi.org/10.1016/j.pain.2013.04.032

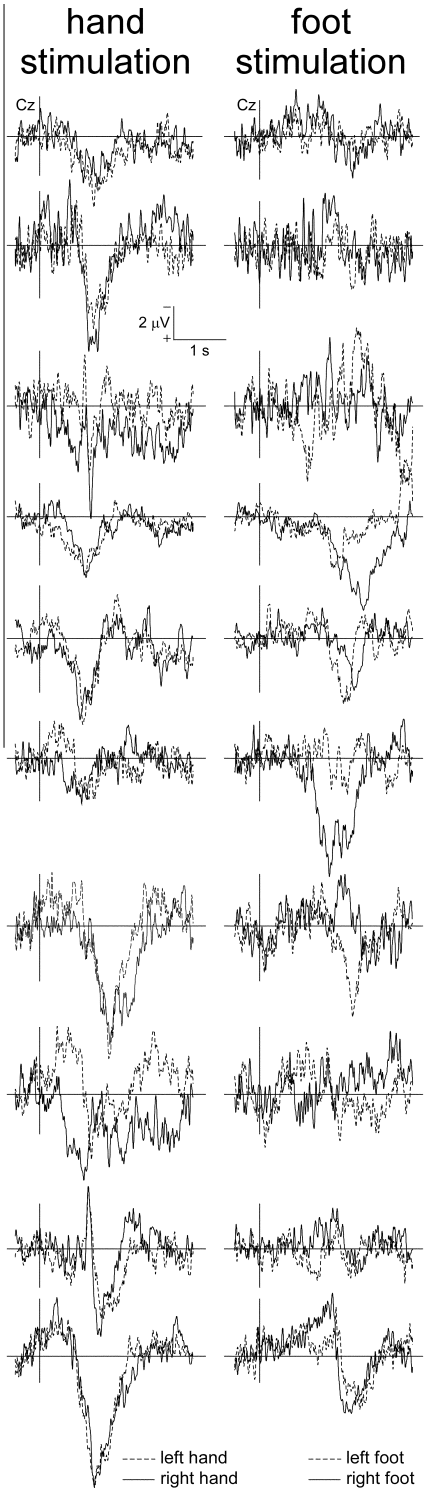

Fig. 2. Single-subject C-fibre laser-evoked potential waveforms obtained at the scalp vertex (electrode Cz) after stimulation of the left (dashed waveforms) and right (continuous waveforms) hand and foot dorsum. Note the negative-positive (N2-P2) complex visible in most waveforms, in particular after stimulation of the hand.

2.7.1. Point-by-point statistical assessment of TF maps

To assess the significance of the relative increases and decreases of signal amplitude observed in the group-level average TF maps, a 1-sample *t* test against zero was performed at each TF point using the ER% amplitudes estimated in each subject. This yielded, for each stimulus location and electrode, a TF map highlighting the regions where the EEG signal deviated significantly from baseline ($P < .05$) (Fig. 6).

2.7.2. Region-of-interest (ROI) analysis

The TF maps were used to arbitrarily define a number of TF ROIs circumscribing the stimulus-induced EEG responses. For each subject, amplitude values of the 10% of pixels exhibiting maximum or minimum amplitude values were averaged and used as summary values estimating response magnitude within each ROI (top x% approach) [12].

2.7.3. Discrimination performance

The analysis was applied using the LEP and NOLEP datasets. For each ROI, the estimates of response magnitude were used to build a receiver-operator characteristic curve assessing the ability of each of these different measures to discriminate between LEP and NOLEP conditions, ie, between the presence vs absence of stimulus-evoked responses. The analysis was performed using Graphpad Prism 5 (Graphpad Software, Inc., La Jolla, CA). The area under the receiver-operator characteristic curve (AUC) was used as an index of discrimination performance. The Youden index was taken as optimal cut-off [11] and used to calculate sensitivity and specificity.

2.7.4. Phase-locking statistics

The wavelet transform was also used to compute TF matrices estimating the degree of phase-locking across trials [15,33]. At each TF bin, phase values were extracted from the wavelet transform of each single trial by computing the argument of the complex wavelet coefficients. These phase values were then used to create, for each trial, a vector having a length of 1 and an angle corresponding to the estimated phase. The phase-locking value was obtained by taking the length of the vector average. This value ranges from 0 (random phases across trials) to 1 (perfect phase alignment across trials) (Fig. 7).

2.8. Supplementary analysis

Three additional datasets were created by assigning trials to 1 of the following 3 categories: (1) undetected trials, (2) trials detected with RTs compatible with the conduction velocity of C-fibres (hand: RT $\geqslant$ 650 ms; foot: RT $\geqslant$ 750 ms), and (3) trials detected with RTs compatible with the conduction velocity of Aδ-fibres (hand: RT < 650 ms; foot: RT < 750 ms). As for the main analyses, the obtained datasets were analysed in the time domain (Fig. 4) and in the TF domain.

3. Results

3.1. Behavioural results

3.1.1. Stimulus detection rate

Using the adaptive stimulation algorithm (Fig. 1), the average rate of detections with RTs compatible with the conduction velocity of C-fibres, ie, late detections, was 69.0% ± 7.0% (hand: RT $\geqslant$ 650 ms, 64.2% ± 16.5%; foot: RT $\geqslant$ 750 ms, 74.3% ± 14.4%).

3.1.2. Target skin temperature

The group-level mean skin temperature at detection with RTs compatible with the conduction velocity of C-fibres was 40.6°C ± 0.4°C after stimulation of the hand and 43.5°C ± 0.1°C after stimulation of the foot. This difference in skin temperature was significant. Indeed, the repeated-measures ANOVA showed a significant main effect of the factor limb (hand vs foot; $F = 17.23$, $P = .002$), no significant main effect of the factor side (left vs right;

Please cite this article in press as: Jankovski A et al. Reliable EEG responses to the selective activation of C-fibre afferents using a temperature-controlled infrared laser stimulator in conjunction with an adaptive staircase algorithm. PAIN® (2013), http://dx.doi.org/10.1016/j.pain.2013.04.032

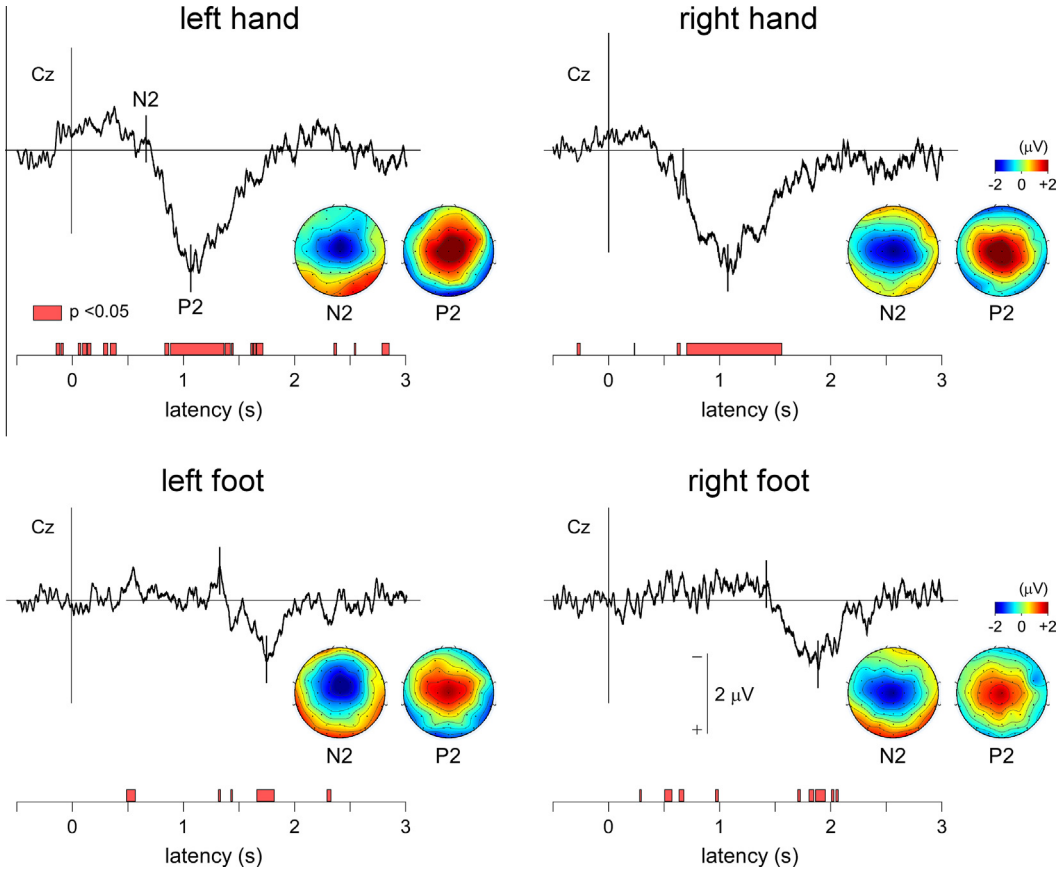

Fig. 3. Group-level average of C-fibre laser-evoked potentials obtained after stimulation of the left and right hand and foot dorsum (electrode Cz). The elicited responses consisted of a late latency negative-positive complex (hand: N2: 704 ± 179 ms, P2: 984 ± 149 ms; foot: N2: 1314 ± 171 ms, P2: 1716 ± 199 ms). As shown in the group-level average scalp maps, both peaks were maximal at the scalp vertex and symmetrically distributed over both hemispheres. A point-by-point *t* test against zero was used to identify the time intervals during which the obtained waveforms differed significantly from baseline (shown in red).

F = 0.78, *P* = .400), and no significant interaction between the 2 factors (F = 0.17, *P* = .690).

3.2. Across-trial averaging in the time domain

As shown in Figs. 2 and 3 and in Table 1, a late-latency negative-positive complex (N2 and P2 waves) was visible in the single-subject and group-level average waveforms obtained after stimulation of the hand and foot. Both peaks were maximal at the scalp vertex and were symmetrically distributed over both hemispheres (Fig. 3). The P2 wave, and even more so the N2 wave, were more clearly identifiable in the average waveforms of the subset of trials detected with RTs compatible with the conduction velocity of C-fibres (Fig. 4).

3.2.1. Visual identification of C-fibre LEPs

The 3 blinded observers were able to consistently distinguish between LEP and NOLEP waveforms, with a high sensitivity (96.7% ± 5.16% after hand stimulation; 78.3% ± 7.5% after foot stimulation) and specificity (98.3% ± 4.1% after hand stimulation; 83.3% ± 10.3% after foot stimulation) (Table 2).

The group-level mean latency of the N2 wave was 704 ± 179 ms after stimulation of the hand dorsum and 1314 ± 171 ms after stimulation of the foot dorsum. The repeated-measures ANOVA revealed a significant main effect of the factor limb (hand vs foot; F = 100.474, *P* = .001), no main effect of the factor side (left vs right; F = 0.021, *P* = .892) and no interaction between the 2 factors (F = 0.281, *P* = .624).

The group-level mean latency of the P2 wave was 984 ± 149 ms after stimulation of the hand dorsum and 1716 ± 199 ms after stimulation of the foot dorsum. As for the N2 wave, the repeated-measures ANOVA revealed a significant main effect of the factor limb (hand vs foot; F = 233.556, *P* = .0001), no main effect of the factor side (left vs right; F = 0.074, *P* = .799), and no interaction between the 2 factors (F = 0.320, *P* = .602).

The group-level mean amplitude of the N2 wave was −1.4 ± 1.7 μV after stimulation of the hand and −2.2 ± 1.3 μV after stimulation of the foot. The group-level mean amplitude of the P2 wave was 4.8 ± 1.8 μV (N2-P2 peak-to-peak amplitude: 6.3 ± 2.6 μV) after stimulation of the hand and 3.0 ± 1.5 μV (N2-P2 peak-to-peak amplitude: 5.2 ± 1.4 μV) after stimulation of the foot. The repeated-measures ANOVA showed no significant effect of limb and side on the baseline-to-peak N2 and P2 amplitudes, and on the peak-to-peak N2-P2 amplitude.

3.2.2. Point-by-point analysis of LEP waveforms

As shown in Fig. 3, the LEP waveforms obtained at electrode Cz deviated significantly and consistently from baseline between approximately 750 and 1500 ms after stimulation of the left and right hand, and between approximately 1500 and 2000 ms after stimulation of the left and right foot.

3.2.3. Point-by-point assessment of hemispheric lateralization

At the latency of the N2 and P2 peaks, the scalp topographies did not show any significant lateralization (Fig. 3). However, when the stimuli were delivered to the left and right hand, the

Please cite this article in press as: Jankovski A et al. Reliable EEG responses to the selective activation of C-fibre afferents using a temperature-controlled infrared laser stimulator in conjunction with an adaptive staircase algorithm. PAIN® (2013), http://dx.doi.org/10.1016/j.pain.2013.04.032

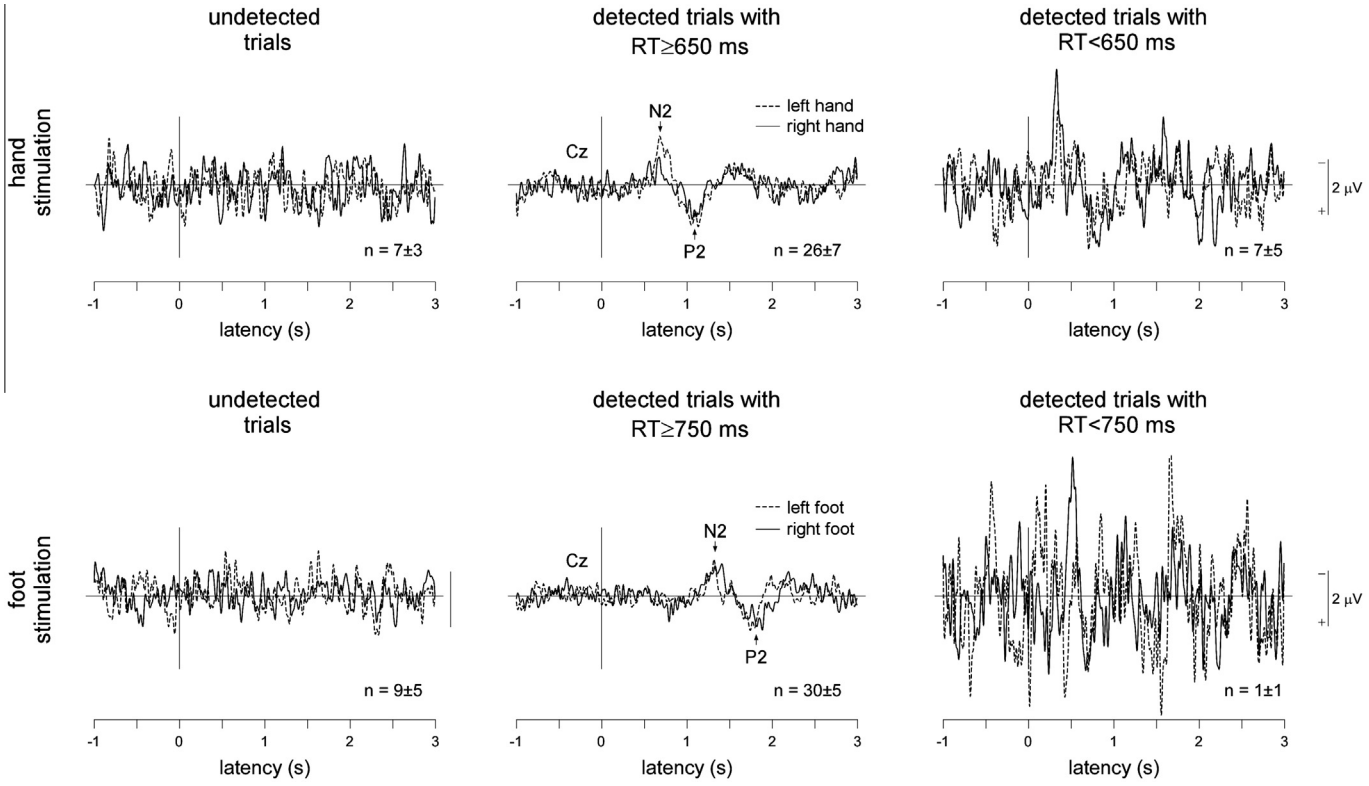

Fig. 4. For each single subject, an additional dataset was obtained by assigning trials to one of the following 3 categories: undetected trials (left panels), trials detected with reaction times (RTs) compatible with the conduction velocity of C-fibres (hand: RT ⩾ 650 ms; foot: RT ⩾ 750 ms; middle panels) and trials detected with RTs compatible with the conduction velocity of Aδ-fibres (hand: RT < 650 ms; foot: RT < 750 ms; right panels). The figure represents the group-level average waveforms obtained at electrode Cz after stimulation of the left (dashed waveforms) and right (continuous waveforms) hand and foot dorsum. Note the small number of undetected trials and trials detected with RTs compatible with the conduction velocity of Aδ-fibres (group-level mean ± SD), explaining the low signal-to-noise ratio of these average waveforms, and due to the adaptive algorithm used to increase the number of trials detected with RTs compatible with the selective activation of C-fibres.

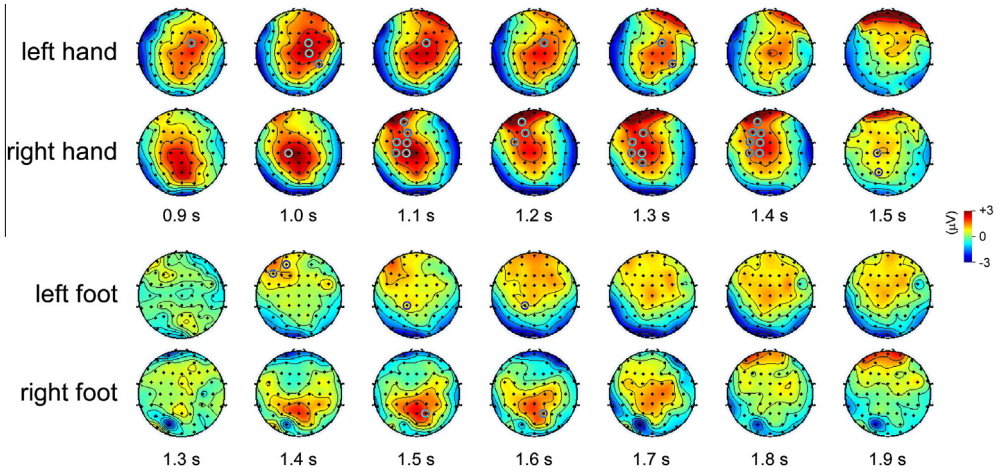

Fig. 5. Point-by-point assessment of the hemispheric lateralization of C-fibre laser-evoked potentials elicited by stimulation of the hand and foot dorsum. For each time point of the average waveforms, paired-sample *t* tests were performed using all pairs of scalp electrodes located left and right from the midline (eg, C1 vs C2; C3 vs C4). Electrodes showing a significantly greater amplitude are highlighted by a circle. The figure represents the group-level average scalp maps (color scale) during the reascending portion of the P2 wave. Note that after stimulation of the hands, signals were significantly greater over the central region contralateral to the stimulated side. Note that this hemispheric asymmetry was not present after stimulation of the foot.

scalp topographies showed a significant and sustained hemispheric lateralization during the reascending portion of the P2 wave. Indeed, during this time interval, the amplitude of the measured signals was greater over the central electrodes contralateral to the stimulated hand. In contrast, such a lateralization of scalp topography was not observed after stimulation of the left and right foot (Fig. 5).

3.3. Across-trial averaging in the TF domain

As shown in the TF maps of average oscillation amplitude (Fig. 6), the TF representation of phase-locked and non–phase-locked EEG responses to the selective activation of C-fibre afferents could be summarised as 3 distinct responses. First, there was a long-lasting enhancement of low frequencies (1 to 5 Hz), extending

Please cite this article in press as: Jankovski A et al. Reliable EEG responses to the selective activation of C-fibre afferents using a temperature-controlled infrared laser stimulator in conjunction with an adaptive staircase algorithm. PAIN® (2013), http://dx.doi.org/10.1016/j.pain.2013.04.032

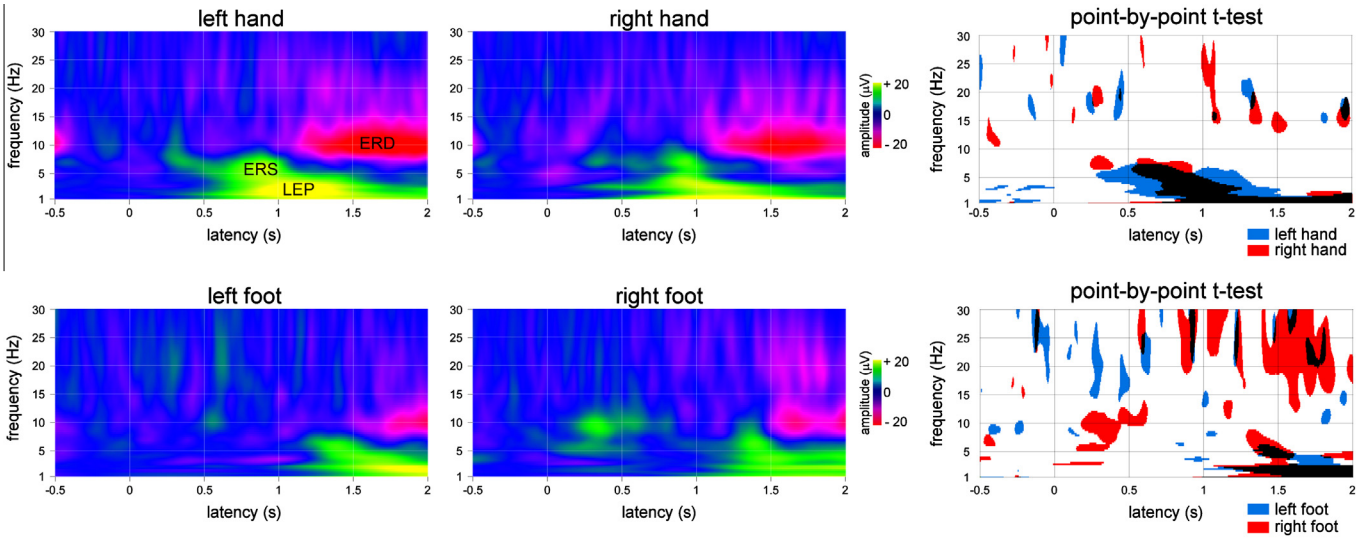

Fig. 6. Left maps. Group-level average of signal amplitude as a function of time (x axis) and frequency (y axis) obtained using the continuous Morlet transform (electrode Cz). Signal increases are represented in yellow, whereas signal decreases are represented in red. The elicited responses could be summarized as (1) a phase-locked enhancement of low frequencies corresponding to the C-fibre laser-evoked potential (LEP), (2) an early and transient non–phase-locked enhancement of higher frequencies (event-related synchronization, ERS), and (3) a late and long-lasting event-related desynchronization of alpha- and beta-band electroencephalogram oscillations (ERD). Right maps. A point-by-point *t* test against zero was used to identify the time-frequency regions during which the obtained maps differed significantly from baseline after stimulation of the left (blue) and right (red) hand and foot.

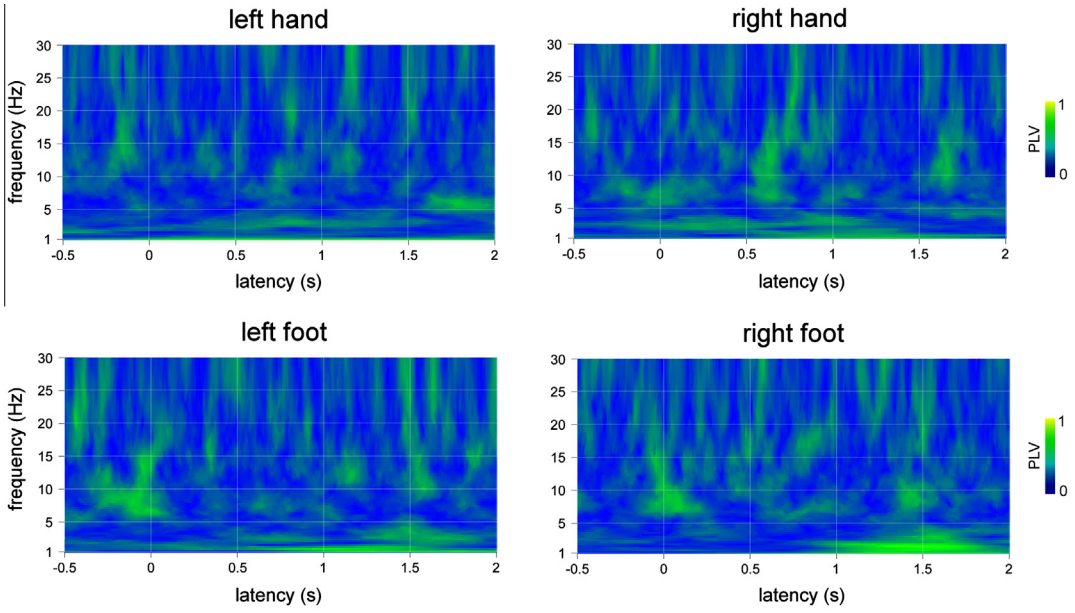

Fig. 7. Phase-locking statistics. The wavelet transform was used to compute time-frequency maps estimating phase-locking across trials (phase-locking value, PLV). Note that the average PLVs at the time-frequency location corresponding to the C-fibre laser-evoked potentials were relatively low, suggesting that an important amount of temporal jitter affects the brain responses to C-fibre input, and hence that time-domain averaging is likely to markedly distort and attenuate the magnitude of C-fibre laser-evoked potentials.

from approximately 700 to 1500 ms after stimulation of the hand and from approximately 1100 to more than 2000 ms after stimulation of the foot. As shown in the TF representation of phase-locking values (Fig. 7), this response showed a certain amount of phase-locking across trials, indicating that it corresponded to the TF representation of the phase-locked LEP. In addition to this phase-locked EEG response, C-fibre input also elicited an early and more transient response at higher frequencies (5 to 10 Hz), centred around 1000 ms after stimulation of the hand and 1500 ms after stimulation of the foot. As shown in the TF representation of phase-locking values, this response was not phase-locked across trials. Finally, C-fibre input induced a long-lasting desynchronisation of alpha- and beta-band EEG oscillations (8 to 25 Hz) starting approximately 1000 ms after stimulation of the hand and approximately 1500 ms after stimulation of the foot.

3.3.1. ROI analysis and discrimination performance

Based on the obtained TF maps, 3 distinct TF ROIs were defined as follows. After stimulation of the hand dorsum, ROI-LEP (2 to 5 Hz; 800 to 1300 ms) circumscribed the phase-locked enhancement of low frequencies, ROI-ERS (5 to 8 Hz; 700 to 1000 ms) circumscribed the earlier and non–phase-locked enhancement of

Please cite this article in press as: Jankovski A et al. Reliable EEG responses to the selective activation of C-fibre afferents using a temperature-controlled infrared laser stimulator in conjunction with an adaptive staircase algorithm. PAIN® (2013), http://dx.doi.org/10.1016/j.pain.2013.04.032

Table 1
Latency and amplitude of C-fibre laser-evoked potentials after stimulation of the hand and foot dorsum.

	Hand	Foot
N2 wave		
Latency (ms)	704 ± 179	1314 ± 171
Amplitude (μV)	−1.4 ± 1.7	−2.2 ± 1.3
P2 wave		
Latency (ms)	984 ± 149	1716 ± 171
Amplitude (μV)	4.8 ± 1.8	3.0 ± 1.5

higher frequencies, and ROI-ERD (7.5 to 13 Hz; 1000 to 2000 ms) circumscribed the late event-related desynchronization of alpha-band EEG oscillations. Similar ROIs were defined to circumscribe the EEG responses after stimulation of the foot: ROI-LEP (2 to 5 Hz; 1300 to 1800 ms), ROI-ERS (5 to 8 Hz; 1100 to 1500 ms), and ROI-ERD (7.5 to 13 Hz; 1500 to 2300 ms). The topographical distribution of the signal measured within ROI-LEP and ROI-ERS were maximal at the scalp vertex, symmetrically distributed over the 2 hemispheres, and similar to the scalp topographies of the N2 and P2 peaks. The topographical distribution of ROI-ERD was slightly more posterior.

At electrode Cz, the magnitude of the activity measured within ROI-LEP was able to efficiently discriminate between LEP and NO-LEP trials. Indeed, and as shown in Fig. 8, the ability of ROI-LEP to discriminate between LEP and NOLEP trials was significant after hand stimulation (AUC = 0.93 ± 0.04; $P < .0001$; sensitivity: 85%, specificity: 90%) and foot stimulation (AUC = 0.81 ± 0.07; $P = .0007$; sensitivity: 80%, specificity: 75%). The discrimination performance of ROI-ERS also was significant after hand stimulation (AUC = 0.89 ± 0.05; $P < .0001$; sensitivity: 80%, specificity: 85%) and foot stimulation (AUC = 0.76 ± 0.08; $P = .0045$; sensitivity: 70%, specificity: 70%). In contrast, the discrimination performance of ROI-ERD was not significant (hand dorsum AUC = 0.62 ± 0.09, $P = .21$; foot dorsum AUC = 0.52 ± 0.10, $P = .87$).

4. Discussion

Reliable EEG responses to the selective activation of C-fibre afferents can be obtained in healthy subjects using temperature-controlled CO_2 laser stimuli delivered to the hand or foot dorsum, in conjunction with an adaptive stimulation algorithm designed to maintain the temperature of the stimuli above the threshold of C-fibre afferents but below the threshold of Aδ-fibre afferents.

The feasibility of recording C-fibre LEPs has already been demonstrated in previous studies [1,2,4,16,19,21,26,28–30,35,38]. However, these approaches have failed to translate into a clinical diagnostic tool because they are difficult to implement and often unreliable. For example, to obtain a selective blockade of myelinated A-fibres using nerve compression, pressure must be maintained for more than 60 minutes [2]. The slightest interruption releases the blockade and requires restarting the entire procedure. Therefore, subjects must absolutely refrain from any movement regardless of discomfort. Also, nerve pressure blocks can only be applied to a few restricted locations, where a sensory nerve is superficial and crosses a bone giving rigid support, thus limiting its potential clinical applications. Similarly, the very small surface areas needed to activate C-fibre afferents selectively are difficult to achieve and maintain constant from trial to trial [1]. Furthermore, the signal-to-noise ratio of the obtained responses is very low. For example, Bragard et al. [1] averaged 600 trials to obtain identifiable C-fibre LEPs. Similarly, Franz et al. [8] collected 196 trials at each stimulation site to examine the diagnostic usefulness of C-fibre LEPs in postherpetic neuralgia. Finally, without the ability to control the target temperature, selectively activating low-threshold C-fibre afferents can be difficult because the temperature reached by the stimulus is not only determined by the power and duration of the laser pulse, but also by the possibly drifting baseline skin temperature, as well as changes in power density, for example due to variations in beam incidence. Finally, intraepidermal electrical stimulation as proposed by Otsuru et al. [30] requires delivering stimuli at very low intensities just above the detection threshold of healthy individuals, and this may be difficult to determine in patients.

Here, we combined 2 factors to improve the reliability of selective C-fibre stimulation. First, we took advantage of a CO_2 laser able to deliver constant-temperature heat pulses by temperature feedback-control of laser power. By improving the reproducibility of the stimuli, this increased the likelihood of bringing the skin temperature above the threshold of C-fibre afferents but below the threshold of Aδ-fibre afferents. Furthermore, unlike other laser stimulators, which exhibit a Gaussian beam profile [31], the spatial distribution of radiative power was uniform across the entire beam, thus allowing a homogenous skin temperature within the entire stimulated area, thereby further increasing the likelihood of selectively activating C-fibre afferents. Second, we used an adaptive staircase algorithm relying on RTs to distinguish between responses related to Aδ- and C-fibres in order to maximise the number of trials in which C-fibres were activated selectively.

Using this approach, we found that reliable C-fibre LEPs can be recorded at the individual level (Fig. 2), both after stimulation of the hand and after stimulation of the foot. Importantly, the 3 blinded observers were able to discriminate between presence and absence of C-fibre LEPs with a high sensitivity (hand: 97% ± 5%; foot: 78% ± 8%) and specificity (hand: 98% ± 4%; foot: 83% ± 10%), thus indicating that our approach could be used to assess C-fibre function in a clinical setting. Such as reported in previous studies [26,36], the latency of the N2 and P2 components elicited by stimulation of the foot (N2: 1314 ± 171 ms; P2: 1716 ± 199 ms) was significantly greater than the latency of the N2 and P2 components elicited by stimulation of the hand (N2: 704 ± 179 ms; P2: 984 ± 149 ms). This difference is easily explained by the greater conduction distance of C-fibre input originating from the foot as compared to C-fibre input originating from the hand. Future studies should examine whether comparison of the latencies of C-fibre LEPs elicited by stimulation of proximal vs distal segments of the same limb, by stimulation of the upper and lower limbs, or by stimulation of the dorsal skin innervated by different dermatomes could be used to obtain reliable

Table 2
Sensitivity and specificity of visual laser-evoked potential identification per observer.

	Right hand		Left hand		Right foot		Left foot	
	Sensitivity (%)	Specificity (%)	Sensitivity (%)	Specificity (%)	Sensitivity (%)	Specificity (%)	Sensitivity (%)	Specificity (%)
Observer 1	100	100	100	100	80	80	70	70
Observer 2	100	100	90	100	90	90	70	100
Observer 3	100	100	90	90	80	80	80	80
Average ± SD	100 ± 0	100 ± 0	93 ± 6	97 ± 6	83 ± 6	83 ± 6	73 ± 6	83 ± 15

Please cite this article in press as: Jankovski A et al. Reliable EEG responses to the selective activation of C-fibre afferents using a temperature-controlled infrared laser stimulator in conjunction with an adaptive staircase algorithm. PAIN® (2013), http://dx.doi.org/10.1016/j.pain.2013.04.032

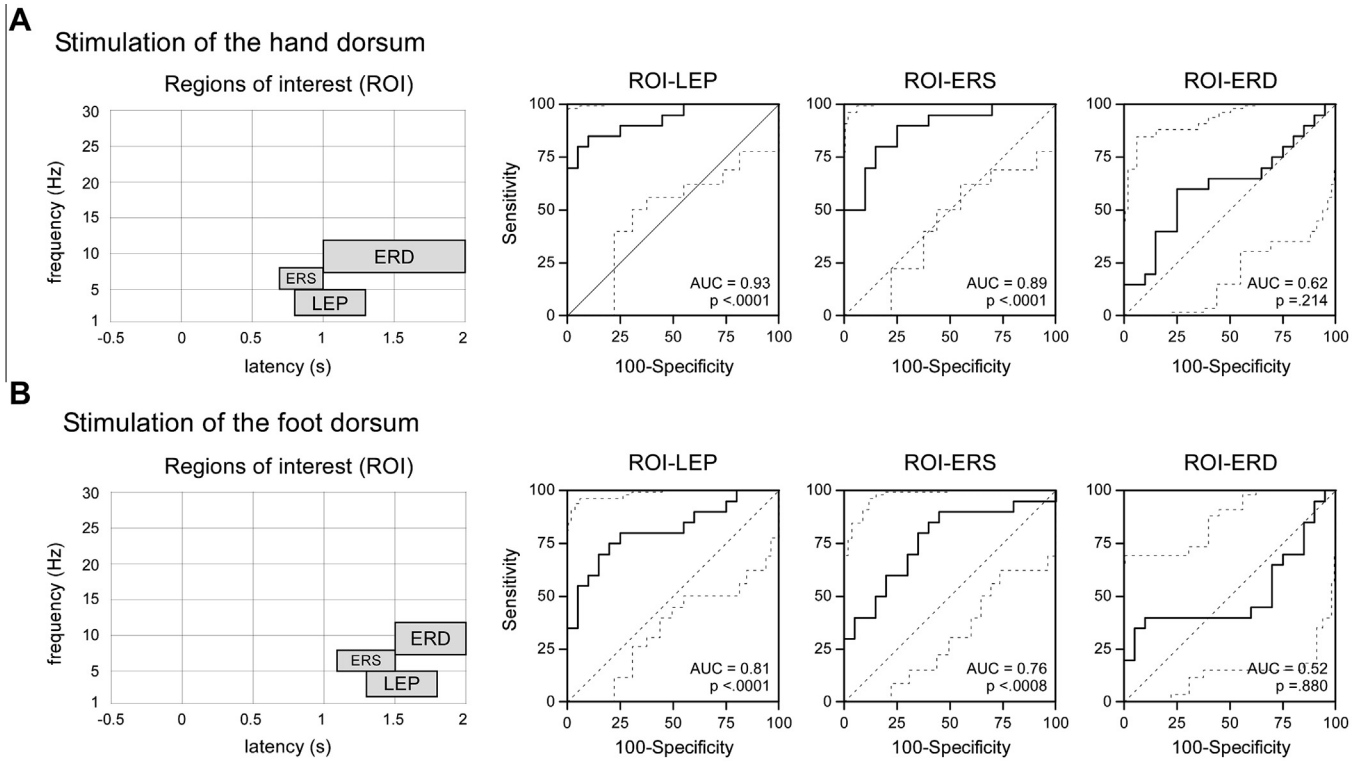

Fig. 8. At electrode Cz, time-frequency regions of interest (ROI) circumscribing three EEG responses were defined for hand (A) and foot (B) dorsum stimulation: ROI-LEP, ROI-ERS and ROI-ERD. For each subject, amplitude values of the 10% of pixels exhibiting maximum (ROI-LEP, ROI-ERS) or minimum (ROI-ERD) amplitude were averaged within each ROI. Receiver Operating Characteristic (ROC) curves were then used to assess the ability of the three measures to discriminate between presence vs. absence of C-fibre stimulation (''LEP'' vs. ''NOLEP''). Note the high area under the curve (AUC) of ROI-LEP and ROI-ERS, in particular, following stimulation of the hand.

estimates of the conduction velocity of peripheral C-fibres and/or spinothalamic tracts [7,14,27,32,36].

Both when stimulating the hand and when stimulating the foot, the scalp topographies of the N2 and P2 peaks were maximal at the scalp vertex and were symmetrically distributed over both hemispheres. In contrast, we found that the reascending portion of the P2 wave (approximately 1000 to 1400 ms after stimulus onset) was significantly lateralised after stimulation of the hand, but not after stimulation of the foot (Fig. 5). Indeed, when stimulating the hand dorsum, the reascending portion of the P2 wave was maximal over the frontal and parietal regions of the hemisphere contralateral to the stimulated hand, and this hemispheric asymmetry was not visible when stimulating the foot dorsum. This finding indicates that the later part of C-fibre LEPs receives a contribution from cortical areas that are somatopically organised. Interestingly, such a lateralisation of the later part of C-fibre LEPs has, in fact, already been reported at 1300 ms [28]. When stimulating the hand dorsum in the present study, participants performed an RT task using a button held in the other hand. Therefore, one should envisage that this lateralisation reflected motor-evoked potentials related to the button press [28]. However, this interpretation is contradicted by the fact that C-fibre LEPs obtained by stimulation of the left and right foot did not show any hemispheric lateralisation, although the participants were asked to perform the RT task using their right hand. Hence, our results indicate that the later part of C-fibre LEPs at least partly reflects activity originating from the somatotopically organised primary somatosensory cortex or the mototopically organised primary motor cortex. Given the late latency of this contribution (RT latencies indicate that the stimulus was perceived before the observed lateralisation), it seems unlikely that it reflected early stages of sensory processing. An interesting possibility could be that it reflected activity originating from the primary motor cortex related to the production of pain-related protective motor responses [34].

The TF analysis of C-fibre evoked EEG responses revealed that, in addition to the phase-locked LEP, which appeared as a long-lasting enhancement of low frequencies (1 to 5 Hz) extending from approximately 700 to 1500 ms after stimulation of the hand and from approximately 1100 to more than 2000 ms after stimulation of the foot (Fig. 6), C-fibre input also induced an early and more transient response at higher frequencies (5 to 10 Hz), centred around 1000 ms after stimulation of the hand and 1500 ms after stimulation of the foot, as well as a long-lasting desynchronisation of alpha- and beta-band EEG oscillations (8 to 25 Hz) starting approximately 1000 ms after stimulation of the hand and approximately 1500 ms after stimulation of the foot. Interestingly the average phase-locking value at the TF location corresponding to the C-fibre LEP was relatively low, in particular after stimulation of the foot. This indicates that an important amount of temporal jitter affects the brain responses to C-fibre input, and hence that time-domain averaging is likely to markedly distort and attenuate the magnitude of C-fibre LEPs. However, and although the TF analysis revealed EEG responses that cannot be identified using conventional time-domain averaging, thus indicating that it may provide a more complete picture of how C-fibre input is represented in the human brain, the ability to discriminate between presence vs absence of C-fibre responses was not markedly improved as compared to the discrimination performance of the analysis performed in the time domain. Future studies performed in patients will thus be required to evaluate the added value of this approach.

Notably, the group level mean target skin temperature to elicit C-fibre detections with RTs compatible with C-fibre conduction velocities was greater at the foot (43.5°C ± 0.1°C) as compared to

Please cite this article in press as: Jankovski A et al. Reliable EEG responses to the selective activation of C-fibre afferents using a temperature-controlled infrared laser stimulator in conjunction with an adaptive staircase algorithm. PAIN® (2013), http://dx.doi.org/10.1016/j.pain.2013.04.032

the hand (40.6°C ± 0.4°C). Compatible with this result, previous studies using contact heat thermodes have shown that the hand is more sensitive than the foot for warm and cold [9]. This could be due to differences in intraepidermal nerve fibre density [5].

In conclusion, we show that reliable C-fibre EEG responses can be obtained after stimulation of the hand and foot using a temperature-controlled CO_2 laser stimulator in conjunction with a simple adaptive staircase algorithm relying on RTs to maintain the stimulus above the threshold of C-fibre afferents but below the threshold of Aδ-fibre afferents. Because the approach is easy to implement and the obtained responses can be identified with a high sensitivity and specificity, our approach could be used as a clinical tool to assess C-fibre function in patients, for example, for the early diagnosis of small-fibre neuropathies or to explore pathophysiological mechanisms underlying visceral pain through stimulation of the skin overlying a referred pain area [39]. Most importantly, because the technique is entirely noninvasive, it would constitute an interesting alternative to skin biopsies and microneurography for the longitudinal assessment of disease progression, or for the evaluation of treatment effect for pharmacological development.

Conflict of interest statement

There are no conflicts of interest to report.

Acknowledgements

The authors contributed to the conception of the Laser Stimulation Device (SIFEC, Belgium) by defining the requirements statement. At present, there is no relationship other than a customer relationship between the authors and the manufacturer. A.M. acknowledges support from a Marie Curie European Reintegration Grant (ERG) and the Belgian National Foundation for Scientific Research (FNRS).

References

[1] Bragard D, Chen AC, Plaghki L. Direct isolation of ultra-late (C-fibre) evoked brain potentials by CO_2 laser stimulation of tiny cutaneous surface areas in man. Neurosci Lett 1996;209:81–4.
[2] Bromm B, Neitzel H, Tecklenburg A, Treede RD. Evoked cerebral potential correlates of C-fibre activity in man. Neurosci Lett 1983;43:109–14.
[3] Bromm B, Treede RD. Nerve fibre discharges, cerebral potentials and sensations induced by CO_2 laser stimulation. Hum Neurobiol 1984;3:33–40.
[4] Bromm B, Treede RD. Human cerebral potentials evoked by CO_2 laser stimuli causing pain. Exp Brain Res 1987;67:153–62.
[5] Chien HF, Tseng TJ, Lin WM, Yang CC, Chang YC, Chen RC, Hsieh ST. Quantitative pathology of cutaneous nerve terminal degeneration in the human skin. Acta Neuropathol 2001;102:455–61.
[6] Churyukanov M, Plaghki L, Legrain V, Mouraux A. Thermal detection thresholds of Adelta- and C-fibre afferents activated by brief CO_2 laser pulses applied onto the human hairy skin. PLoS One 2012;7:e35817.
[7] Cruccu G, Iannetti GD, Agostino R, Romaniello A, Truini A, Manfredi M. Conduction velocity of the human spinothalamic tract as assessed by laser evoked potentials. Neuroreport 2000;11:3029–32.
[8] Franz M, Spohn D, Ritter A, Rolke R, Miltner WH, Weiss T. Laser heat stimulation of tiny skin areas adds valuable information to quantitative sensory testing in postherpetic neuralgia. PAIN® 2012;153:1687–94.
[9] Hagander LG, Midani HA, Kuskowski MA, Parry GJ. Quantitative sensory testing: effect of site and skin temperature on thermal thresholds. Clin Neurophysiol 2000;111:17–22.
[10] Hallin RG, Torebjork HE, Wiesenfeld Z. Nociceptors and warm receptors innervated by C fibres in human skin. J Neurol Neurosurg Psychiatry 1982;45:313–9.
[11] Huart C, Legrain V, Hummel T, Rombaux P, Mouraux A. Time-frequency analysis of chemosensory event-related potentials to characterize the cortical representation of odors in humans. PLoS One 2012;7:e33221.
[12] Iannetti GD, Zambreanu L, Wise RG, Buchanan TJ, Huggins JP, Smart TS, Vennart W, Tracey I. Pharmacological modulation of pain-related brain activity during normal and central sensitization states in humans. Proc Natl Acad Sci U S A 2005;102:18195–200.
[13] Jung TP, Makeig S, Westerfield M, Townsend J, Courchesne E, Sejnowski TJ. Removal of eye activity artifacts from visual event-related potentials in normal and clinical subjects. Clin Neurophysiol 2000;111:1745–58.
[14] Kakigi R, Shibasaki H. Estimation of conduction velocity of the spino-thalamic tract in man. Electroencephalogr Clin Neurophysiol 1991;80:39–45.
[15] Lachaux JP, Rodriguez E, Martinerie J, Varela FJ. Measuring phase synchrony in brain signals. Hum Brain Mapp 1999;8:194–208.
[16] Lankers J, Frieling A, Kunze K, Bromm B. Ultralate cerebral potentials in a patient with hereditary motor and sensory neuropathy type I indicate preserved C-fibre function. J Neurol Neurosurg Psychiatry 1991;54:650–2.
[17] Lewis T, Pochin EE. The double pain response of the human skin to a single stimulus. Clin Sci 1937;3:37–67.
[18] Lopes da Silva FH, Pfurtscheller G. Basic concepts on EEG synchronization and desynchronization. Event-related desynchronization and related oscillatory phenomena of the brain. In: Lopes da Silva FH, editor. Handbook of electroencephalography and clinical neurophysiology. Amsterdam: Elsevier; 1999. p. 3–11.
[19] Magerl W, Ali Z, Ellrich J, Meyer RA, Treede RD. C- and A delta-fiber components of heat-evoked cerebral potentials in healthy human subjects. PAIN® 1999;82:127–37.
[20] Meyer RA, Walker RE, Mountcastle Jr VB. A laser stimulator for the study of cutaneous thermal and pain sensations. IEEE Trans Biomed Eng 1976;23:54–60.
[21] Mouraux A, Guerit JM, Plaghki L. Non-phase-locked electroencephalogram (EEG) responses to CO_2 laser skin stimulations may reflect central interactions between A partial partial differential- and C-fibre afferent volleys. Clin Neurophysiol 2003;114:710–22.
[22] Mouraux A, Iannetti GD. Across-trial averaging of event-related EEG responses and beyond. Magn Reson Imaging 2008;26:1041–54.
[23] Mouraux A, Plaghki L. Are laser-evoked brain potentials modulated by attending to first or second pain? PAIN® 2007;129:321–31.
[24] Nahra H, Plaghki L. The effects of A-fiber pressure block on perception and neurophysiological correlates of brief non-painful and painful CO_2 laser stimuli in humans. Eur J Pain 2003;7:189–99.
[25] Ochoa J, Mair WG. The normal sural nerve in man. I. Ultrastructure and numbers of fibres and cells. Acta Neuropathol 1969;13:197–216.
[26] Opsommer E, Guerit JM, Plaghki L. Exogenous and endogenous components of ultralate (C-fibre) evoked potentials following CO_2 laser stimuli to tiny skin surface areas in healthy subjects. Neurophysiol Clin 2003;33:78–85.
[27] Opsommer E, Masquelier E, Plaghki L. Determination of nerve conduction velocity of C-fibres in humans from thermal thresholds to contact heat (thermode) and from evoked brain potentials to radiant heat (CO_2 laser). Neurophysiol Clin 1999;29:411–22.
[28] Opsommer E, Weiss T, Miltner WH, Plaghki L. Scalp topography of ultralate (C-fibres) evoked potentials following thulium YAG laser stimuli to tiny skin surface areas in humans. Clin Neurophysiol 2001;112:1868–74.
[29] Opsommer E, Weiss T, Plaghki L, Miltner WH. Dipole analysis of ultralate (C-fibres) evoked potentials after laser stimulation of tiny cutaneous surface areas in humans. Neurosci Lett 2001;298:41–4.
[30] Otsuru N, Inui K, Yamashiro K, Miyazaki M, Ohsawa N, Takeshima Y, Kakigi R. Selective stimulation of C fibers by an intra-epidermal needle electrode in humans. Open Pain J 2009;2:53–6.
[31] Plaghki L, Mouraux A. How do we selectively activate skin nociceptors with a high power infrared laser? physiology and biophysics of laser stimulation. Neurophysiol Clin 2003;33:269–77.
[32] Qiu Y, Inui K, Wang X, Tran TD, Kakigi R. Conduction velocity of the spinothalamic tract in humans as assessed by CO(2) laser stimulation of C-fibers. Neurosci Lett 2001;311:181–4.
[33] Rodriguez E, George N, Lachaux JP, Martinerie J, Renault B, Varela FJ. Perception's shadow: long-distance synchronization of human brain activity. Nature 1999;397:430–3.
[34] Schulz E, Tiemann L, Witkovsky V, Schmidt P, Ploner M. Gamma oscillations are involved in the sensorimotor transformation of pain. J Neurophysiol 2012;108:1025–31.
[35] Terhaar J, Viola FC, Franz M, Berger S, Bar KJ, Weiss T. Differential processing of laser stimuli by Adelta and C fibres in major depression. PAIN® 2011;152:1796–802.
[36] Tran TD, Inui K, Hoshiyama M, Lam K, Kakigi R. Conduction velocity of the spinothalamic tract following CO_2 laser stimulation of C-fibers in humans. PAIN® 2002;95:125–31.
[37] Treede RD, Meyer RA, Raja SN, Campbell JN. Evidence for two different heat transduction mechanisms in nociceptive primary afferents innervating monkey skin. J Physiol 1995;483:747–58.
[38] Truini A, Galeotti F, Cruccu G, Garcia-Larrea L. Inhibition of cortical responses to Adelta inputs by a preceding C-related response: testing the "first come, first served" hypothesis of cortical laser evoked potentials. PAIN® 2007;131:341–7.
[39] Wilder-Smith CH, Song G, Yeoh KG, Ho KY. Activating endogenous visceral pain modulation: a comparison of heterotopic stimulation methods in healthy controls. Eur J Pain 2009;13:836–42.